Fabric Thermal Display using Ultrasonic Waves

Haokun Wang*
The University of Texas at Dallas

Yatharth Singhal†
The University of Texas at Dallas

Jin Ryong Kim‡
The University of Texas at Dallas

Figure 1: (a) Different types of thermal displays used, (b) a user interacting with the virtual environment while wearing the thermal glove, and (c) user's point of view.

Abstract

This paper presents a fabric-based thermal display of a polyester fabric material combined with thermally-conductive materials using an ultrasound haptic display. We first empirically test the thermal generation process in five fabric materials by applying 40 kHz ultrasonic waves to the fabric materials. We also examine their thermal characteristics by applying different frequencies and amplitudes of ultrasonic cues. We show that polyester demonstrates the best thermal performance. We then combine it with thermally-conductive materials, including copper and aluminum, and compare them with the fabric-only condition. Two user studies show that our approach of combining a fabric material with copper and aluminum outperforms fabric-only conditions in thermal perception and thermal level identification. We integrate polyester with aluminum into a glove to explore the use cases in VR and share our findings, insights, limitations, and future works.

Index Terms: Haptics—Thermo-tactile Feedback—VR—

1 Introduction

Providing thermal feedback becomes essential to enrich the user experience as high-fidelity, multi-sensory cues are vital in increasing presence and immersion in today's virtual environments. Recent studies [1–8] have shown that thermal feedback, when integrated into the VR environment, can increase immersion and realism significantly.

Wearable thermal actuators using Peltiers are widely used to provide thermal sensations [9–12]. The thermoelectric effect creates a heat flux between two materials, usually N-type and P-type semiconductors, which are attached on two sides of Peltier's ceramic substrate and results in hot on one side and cold on another side [13]. The fast thermal response time and wide temperature range made Peltier a powerful thermal device. At the same time, the energy consumption is high, and the direct current-driven device requires a complicated low voltage high current converter for precise control. An extra circulation system was needed to provide thermal equilibrium on the unused side [14]. The overall size of Peltier based thermal system is relatively large, and most of the components are rigid body and heavy, which makes it bulky for a user to wear and hinders natural body movement.

Another common approach is liquid-based wearable thermal display [15,16]. The liquid (usually water) is heated to a specific temperature level and circulated within the thermal display, transferring heat to the skin through a water tube. With high specific heat capacity, water could maintain the temperature of the thermal display at a stable range within a relatively large area [15]. However, the water tube must be connected to the pump and heating source, which drastically enlarges the system size. Also, the water becomes too heavy when the size of the thermal display is increased, making it difficult for thermal interaction. The non-contacted thermal displays are also widely used using hot airflow [17,18], infrared [19], and laser [20], but it's difficult to achieve localized thermal sensations due to the diffusion of air and unidirectional feature of infrared wave [17,19]. Also, the thermal convection and radiation would attenuate with range, making it hard to provide stimulus to different body parts [20].

Our approach is based on recent studies [21–23], which use airborne ultrasound phased arrays to generate heat on the cotton fabric. In their studies, they discovered a thermal phenomenon that heat is generated through sound absorption when the cotton fabric absorbs the heat energy from the ultrasound waves and provides a thermal effect on the palm through heat conduction. They observed that the stimulated fabric area (a region where ultrasound tactile cues were presented) reached a significantly higher temperature than the non-stimulated area.

The ultrasound phased array uses multiple transducers to concentrate sound energy in a limited area in 3D space, i.e., focal point, by phase and amplitude control of each transducer [24, 25]. When the focal point is modulated within the skin mechanoreceptor perception range between 100 and 200Hz, the ultrasound display can provide tactile feedback

*e-mail: Haokun.Wang@utdallas.edu
†e-mail: Yatharth.Singhal@utdallas.edu
‡e-mail: Jin.Kim@utdallas.edu

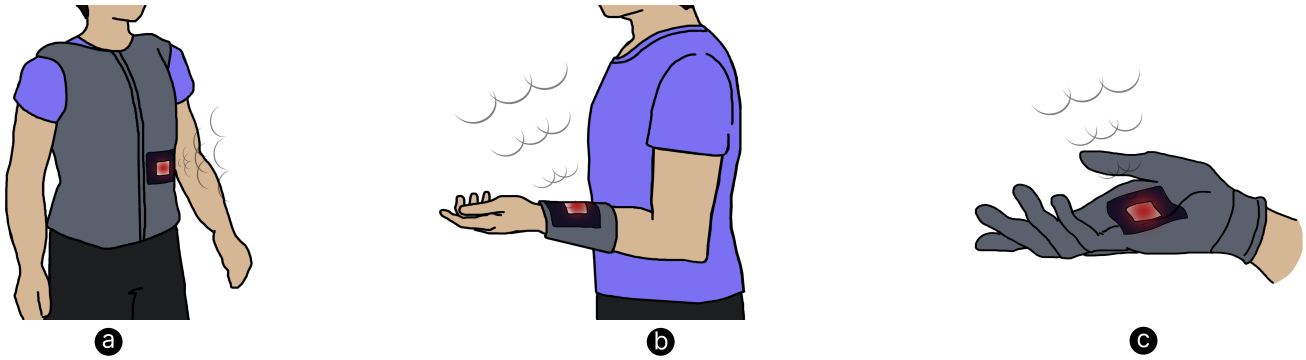

Figure 2: Possible applications of our approach: (a) A thermal vest, (b) thermal armband, and (c) thermal glove.

on the human body. The ultrasound phased array is generally used for providing tactile stimuli. However, as those previous studies [21–23] demonstrated, the acoustic energy of the focal point could also be transferred into heat through absorptive material, which could be applied to provide thermal sensation. The array can also provide cold sensation by ultrasound-driven mist vaporization [26]. The acoustic energy carried by the sound wave would be absorbed when the wave propagates from air into an absorptive material, where most waves transformed into heat, and less wave got reflected [27]. Many factors influence absorption performance, such as thickness, density, porosity, etc. [28]. Fibrous materials with porous structures are widely used in acoustic energy absorption, including natural fiber, synthetic fiber, and metallic fiber [28, 29]. The commonly used fabrics, mainly made of natural and synthetic fiber, could be used as an easy-to-get and effective acoustic energy absorption material.

This paper extends their previous thermal studies [21–23] by proposing fabric-based thermal displays with ultrasonic waves and thermally conductive materials. Their studies showed that a promising temperature could be achieved on the fabric using ultrasound waves, but the human thermal perception was not clearly observed. Although a significantly high temperature of heat was generated in the fabric, most of the heat energy would be transferred to the exposed air, yielding poorly noticeable thermal sensations. Our approach uses thermally-conductive materials to transfer the absorbed heat energy to keep and deliver the thermal sensations to the human skin. Integrating thermally-conductive materials is necessary, as the fabric materials have low thermal conductivity. The fabric must be tightly in contact with the skin to ensure effective heat conduction, while the thermally-conductive material could provide clear thermal stimuli with slight contact. Also, due to the limited cue size of the ultrasound display (usually 10 mm or 20 mm in diameter), the perceivable area is small, while the thermally-conductive material could expand this area for better thermal perception. We confirmed that thermal sensations are barely perceivable without integrating thermally-conductive material, as shown in our user studies.

In this paper, we propose a fabric-based thermal display that uses fabric with thermally-conductive materials and an external, non-contact energy source of ultrasound haptic display (see Figure 1). We show the thermal characteristics of different fabric materials (i.e., polyester, rayon, cotton, wool-polyester, and polypropylene) with different amplitudes and frequencies of the focused ultrasound haptic cues. We then select polyester as a good candidate for absorbing heat sensations into the fabric material and build our thermal displays by integrating thermally-conductive materials (i.e., copper and aluminum) to transfer the absorbed heat energy to store and deliver thermal sensations to the human skin. We further demonstrate the feasibility of our approach of integrating fabric with thermally-conductive materials by comparing it with the fabric-only display. This unique approach is compelling as it does not require additional hardware attached to the wearables, allowing users to freely grasp and manipulate thermal objects while experiencing thermal sensations (e.g., thermal gloves). Since this is made of fabric, it can be easily deployed on different body parts (see Figure 2).

2 Thermal Characteristics of Fabric Materials

In this section, we discuss the thermal generation process through mathematical deduction and then conduct the fabric material test to investigate their thermal characteristics when the ultrasound waves are applied.

2.1 Thermal Generation Process

Thermal generation on fibrous materials through acoustic energy absorption has been studied in the noise reduction field. Due to the porous structure of the fibrous materials with good sound absorption coefficient, the sound wave energy can be converted into heat [28].

$$\alpha = \frac{E_a}{E_i} \tag{1}$$

where α denotes sound absorption coefficient, E_i denotes incident sound energy and E_a denotes absorbed sound energy. For porous materials, the α can be estimated with the equation below:

$$\alpha = 1 - \left| \frac{Z - \rho_0 c_0}{Z + \rho_0 c_0} \right| \tag{2}$$

$$Z = Z_0 coth(\gamma l) \tag{3}$$

where Z denotes surface characteristic impedance, ρ_0 denotes air density and c_0 denotes sound velocity, Z_0 denotes characteristic impedance, γ denotes propagation coefficient and l denotes thickness. [28, 30]. Those fibrous materials can be used as a medium to provide thermal sensation at the ultrasound display focal point stimulated area, where the fibrous material absorbs sound energy and causes a temperature increase within that area. The acoustic impedance can be calculated based on empirical model [30] where two main indexes are considered, characteristic impedance

$Z_0 = R + jX$ and propagation coefficient $\gamma = \alpha + j\beta$, where j represents an imaginary number.

The porous material can effectively absorb acoustic energy ($\alpha > 0.8$) within short thickness under the high acoustic frequency (40kHz) and then transfer the acoustic energy to the heat [31]. With the constant acoustic power generated from the phased array Q_A, the absorbed power Q_f is

$$Q_f = \alpha \times Q_A \tag{4}$$

The absorbed heat is then transferred to the top surface of the material to be in contact with the skin.

The thermal process can be explained using the Foster RC thermal equivalent circuit [32], where the power source (i.e., an acoustic array) is connected to the RC circuit (i.e., material) and then connected to R_H and C_H (i.e., the skin), as shown in Figure 3. In this thermal circuit, the V_{in} indicates the temperature of the material's bottom surface, R indicates the inverse thermal conductivity of the material, C indicates the heat capacity of the material, V_{out} indicates the temperature of material's top surface, R_H indicates the inverse thermal conductivity of the human skin and C_H indicates the heat capacity of the human skin.

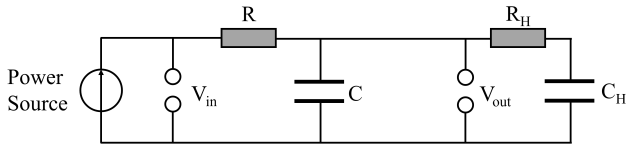

Figure 3: Equivalent thermal circuit of the system.

The heating process can be described as follows: First, the power source heats the material's bottom surface through acoustic wave absorption, resulting in temperature rise (i.e., voltage increase of V_{in}). Then, the heat is transferred to the material's top surface through heat conduction, which can be represented as the current flows from V_{in} passing the RC circuit, where part of the heat is lost due to thermal resistance R and remaining heat charged material's capacitance C, resulting in a temperature increase of V_{out}. After that, the heat is transferred to the user through contact between the material's top surface and skin, representing the heat capacitance of C_H getting charged by C. The charging period can be given as follows:

$$V_{out} = V_{in}(1 - e^{-t/RC}) \tag{5}$$

where the time constant RC indicates the temperature-changing time of the material. The thermal conductivity of the material $\frac{1}{R}$ is determined by the area of the material A and the depth of the material x, which can be given as:

$$Q_f = -\frac{1}{R} A \frac{dV_{out}}{dx} \tag{6}$$

The amount of heat stored and the temperature-changing time of the material can be determined by the type and size of the material.

2.2 Fabric Material Test

We tested different fabric materials to investigate the thermal characteristics when the ultrasound waves were applied. Five porous fabrics were selected based on their density, specific heat, and thermal conductivity as shown in Table 1: cotton, polyester, polypropylene, rayon, and wool-polyester,

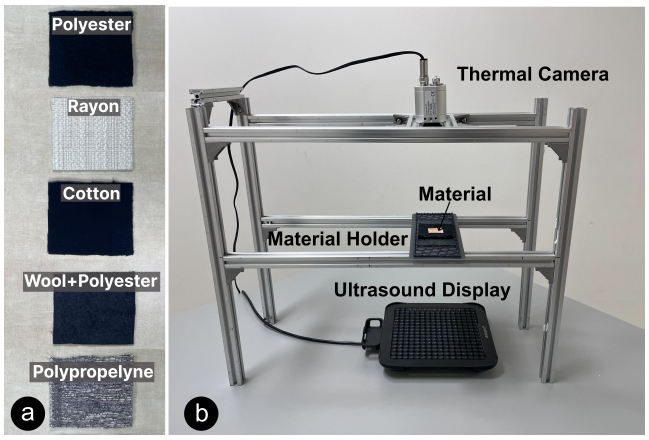

Figure 4: (a) Five selected materials and (b) setup.

with a size of 60 mm (Length) × 60 mm (Width) × 2 mm (Thickness), as shown in Figure 4 (a). The time point stream (TPS) modulation is used for generating focal points due to its higher energy intensity and faster position-changing rate compared to the amplitude modulation (AM) mode.

Setup. Figure 4 (b) shows our test setup. Using aluminum beam frames, we built a supporting structure (540 mm (Length) × 180 mm (Width) × 500 mm (Thickness)) to hold the fabric materials and thermal camera. The ultrasound display (Ultraleap Stratos Explore) was placed at the bottom of the structure, providing a focal point onto the fabric material 200 mm above it. The material holder was 3D printed with a size of 180 mm × 70 mm × 5 mm and a 50 mm × 50 mm hollow structure at the center, placed at a distance of 200 mm above the surface of ultrasound display with geometrical center vertically aligned. A thermal camera (PI450, Optris infrared measurements) was placed at a distance of 190 mm above the material holder to record the temperature change on the fabric material. No cooling effect was observed as we directly emitted ultrasound cues to the bottom of the surface.

Table 1: Materials and their physical features

Materials	Density ρ (kg/m^3)	Specific Heat C (J/kg.K)	Thermal Conductivity K (W/m.K)
Polyester	1200	1.1	0.14
Rayon	1530	1.5	0.026
Cotton	450	1.34	0.065
Wool-polyester	120	1.7	0.047
Poly-propylene	900	1.7	0.2

Conditions. We chose four amplitude levels: 25%, 50%, 75% and 100% of the maximum ultrasound display amplitude level, and four frequency conditions: 50Hz, 100Hz, 200Hz, and 40kHz, at which the focal point is modulated, yielding a total of 16 conditions.

Procedure. Each fabric material was placed at the center of the material holder and fixed with four tapes on the edges. Before each trial, the test material was naturally cooled down until it reached thermal equilibrium at room temperature (23.5°C). When the trial began, the ultrasound display was activated to generate a circle cue with a diameter of 10 mm at the center of the test material for 90 seconds and then turned off. Meanwhile, the thermal camera

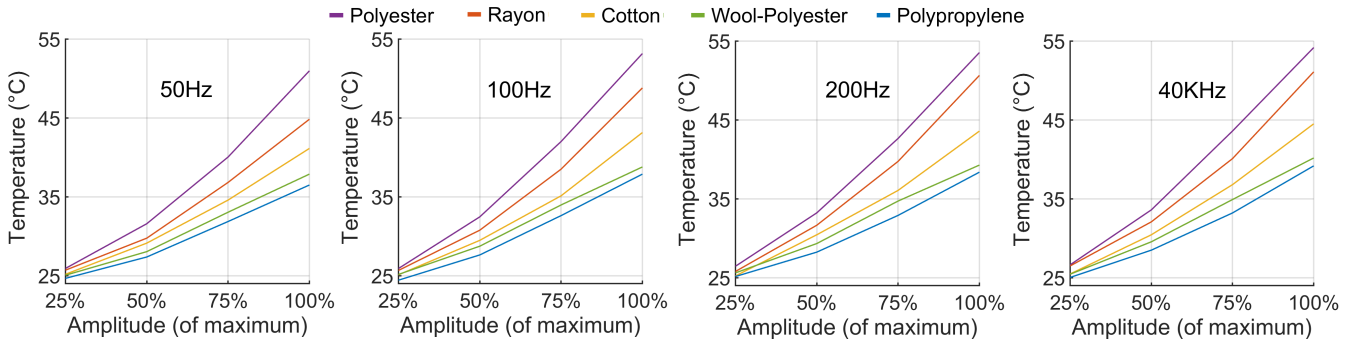

Figure 5: Mean steady-state temperature within acoustic cue area of different materials under different frequencies and amplitude.

recorded the temperature of the area where the focal point was covered during the entire measurement time (until the material was cooled down to room temperature).

2.3 Results

Figure 5 shows the mean temperature changes on the focal point covered area for five materials under different amplitudes. We observed positive correlations between the temperature and amplitude in all five materials, showing higher amplitude yields more sound energy absorbed by the material and converted to a higher temperature. Conversely, the frequency didn't significantly impact the temperature in any of the materials, which matched the characteristics of the TPS modulation mode where applied power is almost the same under different frequencies. Although the 40kHz without modulation mode carried more energy and could reach a higher temperature, the temperature difference is relatively small for 200Hz and 40kHz. We also found that polyester could reach the highest temperature, followed by rayon and cotton across all four frequencies.

3 Proposed Approach

3.1 Design

In previous approaches [21, 23], they demonstrated that the fibrous material could sufficiently absorb sound energy to generate heat. However, the heat transfer from the material to the skin was not effective due to the nature of the low thermal conductivity in the fabric material. The air between the fabric and the skin further reduces the thermal transfer efficiency, resulting in poor thermal perception. Furthermore, the thermal dispersion of the fabric is poor due to its weak thermal conductivity, limiting the thermal area. Our approach is simple. We tightly integrate thermally-conductive materials like copper and aluminum to efficiently improve the heat transfer from the fabric material to the skin. These metal materials can increase the display's overall thermal capacity (385 $J/kg.K$ for copper and 887 $J/kg.K$ for aluminum while 1.1 $J/kg.K$ for polyester) and enlarge the amount of heat that can be supplied, resulting in the temperature to be felt more easily. Once the material is fully charged, i.e., reached the steady state, its contact with the skin would achieve a steep temperature change. Copper is an excellent conductor of heat and is good for heat exchanges and heat sinks (thermal conductivity: 398 W/mK), and aluminum is also known to be a great conductor of heat (thermal conductivity: 251 W/mK). Generally, it is known that copper is more thermally-conductive than aluminum. However, aluminum is more affordable than copper due to its lower production cost.

We used four pieces of polyester with a size of 60 mm (length) × 60 mm (width) × 2 mm (thickness) to design four thermal displays with two different sizes of copper and aluminum (20 mm × 20 mm × 0.09 mm (thickness) and 40 mm × 40 mm) × 0.09 mm (thickness) to validate our approach and evaluate thermal characteristics, namely, $FabCu_{20\times20}$, $FabCu_{40\times40}$, $FabAl_{20\times20}$, and $FabAl_{40\times40}$. Copper and aluminum sheets were tightly attached to the fabric using thermal tape.

3.2 Thermal Performance

We measured the thermal performance of four thermal displays that we designed. We used the same setup (see Figure 4) in Section 2.2 and captured the thermal image of the entire thermal display area, including metal and fabric. We used high-emissivity acrylic black ink to cover the reflective metal surface for an accurate temperature measurement. We set 100% of the maximum amplitude with a 200 Hz modulated frequency with 10 mm and 20 mm diameter of acoustic ultrasonic cue sizes, yielding eight conditions. The procedure was the same as Section 2.2.

Figure 6 shows the thermal image of four displays after reaching stable temperature, where the white circle denotes the contour of the focal point. It is clearly observed that both $FabCu_{20\times20}$ and $FabAl_{20\times20}$ showed higher thermal conductivity, regardless of the size of the cues, as compared to $FabCu_{40\times40}$ and $FabAl_{40\times40}$ (larger size). Figure 7 shows the mean temperatures for four displays with two cue sizes. It clearly shows that both $FabCu_{20\times20}$ and $FabAl_{20\times20}$ with 10 mm of cue size reached the highest temperature.

3.3 Thermal Control

To further explore the controllability of the proposed approach, we measured the thermal characteristics. We selected three thermal displays to measure using polyester fabric: i) *FabOnly*, ii) $FabCu_{20\times20}$, and iii) $FabAl_{20\times20}$. *FabOnly* is a polyester fabric material with no thermally-conductive material attached. We used 25%, 50%, 75%, and 100% of the amplitude of the ultrasound cues with 200 Hz frequency. The procedure was the same as Section 2.2.

Figure 8 shows the mean temperature changes on the stimulated area of three thermal displays under different amplitude levels with 200 Hz frequency. We observed that the temperature of all three displays has a similar trend: higher amplitude yields higher temperature. With 100% amplitude, all three displays exceed the heat-pain detection threshold (43.0°C to 46.8°C), and under 75% amplitude, all three displays exceed the warm detection threshold (32.5°C

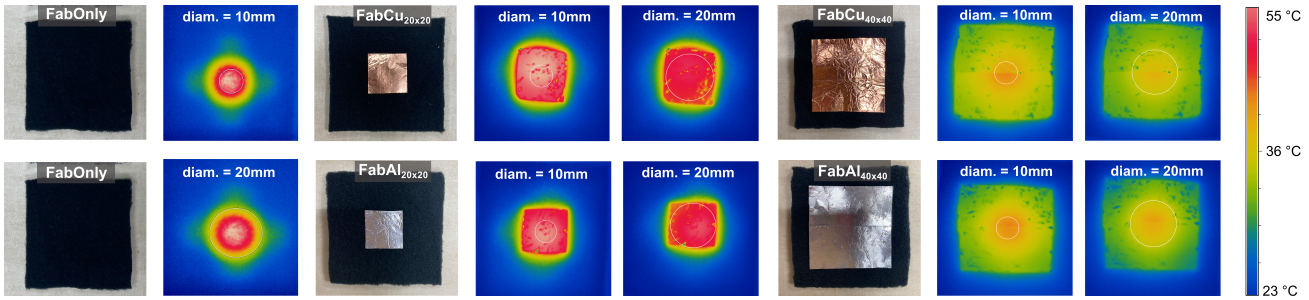

Figure 6: Fabric thermal displays with fabric-only baseline and different sizes of thermally-conductive materials and their thermal distribution.

to 36.7°C) [33]. The stable temperature (after 60 seconds) for $FabAl_{20\times20}$ and $FabCu_{20\times20}$ under all amplitude conditions has a trivial difference (less than 1°C) while lower than the *FabOnly* display.

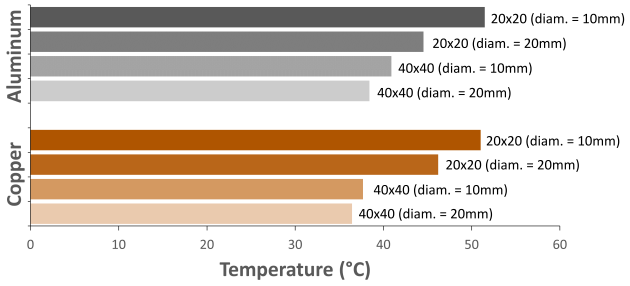

Figure 7: Thermal characteristics of four displays. (a) Polyester fabric with aluminum and (b) Polyester fabric with copper.

4 User Studies

We designed and conducted user studies to compare our proposed approach with the fabric-only baseline condition. We used the same setup used in Section 2.2 for both user studies, and the temperature on the display surface was monitored using a thermal camera. In addition, a set of noise-cancellation headphones were used to play pink noise to block participants from exterior noise. Both studies were approved by the author's institution's Institutional Review Board at the authors' institution.

4.1 User Study 1: Thermal Perception

The goal of this study is to demonstrate the participants' thermal perception of fabric displays, including our approach.

Participants. Twelve participants were recruited for this study (6 females; mean age = 24.6 years old; SD = 2.4 years old). All of them were right-handed, and none reported any disorder affecting the sensations of their hands. Each participant was paid a $10 gift card for their participation.

Experimental Conditions. We selected and compared three polyester thermal displays: Fabric only (*FabOnly*), Fabric with a copper material (20 mm × 20 mm) attached at the center of the fabric ($FabCu_{20\times20}$), and Fabric with an aluminum material (20 mm × 20 mm) attached at the center of the fabric ($FabAl_{20\times20}$). For each condition, thermal displays were exposed to the ultrasound display for 60 seconds to ensure it reached its steady state (i.e., initial charging). We used thermal tape to attach copper and aluminum to the polyester fabric.

Procedure. Participants were briefed about the experimental procedure before starting the experiment. At the beginning of each trial, their initial skin temperature was measured to ensure that the skin temperature returned to normal after the previous trial. The fabric was placed on top of the material holder at a distance of 200 mm from the ultrasound display. A focal point of diameter 10 mm was created in the center of the display. The ultrasound display was set to a frequency of 200 Hz, and maximum amplitude was activated till the temperature of the display stabilized (54.0°C for *FabOnly*, 51.0°C for $FabCu_{20\times20}$, and 51.5°C for $FabAl_{20\times20}$). Participants were asked to place the index finger of their dominant hand inside the white square marked on each display (stimulated area) for 5 seconds, which would be adequate time for thermal perception [34,35]. They were then asked to lift their finger and rate the perceived thermal sensation by asking the following question: *How would you rate the perceived thermal stimulus in terms of intensity?*, using a Visual Analog Scale (VAS). We used the temperature scale ranging from "Neutral" to "Very Hot" which was inspired by Bird et al. [36]. Before the subsequent trial, the ultrasound display was deactivated so that the display could reach back to room temperature (23.5°C for all displays). Each condition was repeated five times, resulting in a total of 15 trials, and the order of the trials was randomized using Latin squares. They were given a post-experiment questionnaire, asking them to rate the clarity of thermal sensation: *I felt thermal sensation clearly while taking trials.* of all three displays on a Visual Analog Scale (VAS), ranging from "Strongly Disagree" to "Strongly Agree". They were also asked to provide their experience through subjective responses. The duration of the experiment was about 60 minutes for each participant. The room temperature was maintained at 23.5°C.

Results and Discussion. Figure 9 (a) shows the perceived thermal stimulus intensity ratings for *FabOnly*, $FabCu_{20\times20}$, and $FabAl_{20\times20}$. The mean perception ratings were 1.71, 4.94, and 5.54 for *FabOnly*, $FabCu_{20\times20}$ and $FabCu_{20\times20}$, respectively. Shapiro-Wilk test showed that the input data was not following a normal distribution. Kruskal–Wallis test followed by a post-hoc Conover test revealed that *FabOnly* had significant differences from both $FabCu_{20\times20}$ ($p < 0.001$) and $FabAl_{20\times20}$ ($p < 0.001$). Although the mean value of the perceived rating for $FabAl_{20\times20}$ was higher than that of $FabCu_{20\times20}$, no significant differences were found between them ($p = 0.06$).

Participants' continuous-scale ratings for thermal clarity were collected and linearly scaled from 0 to 10 (0: Strongly

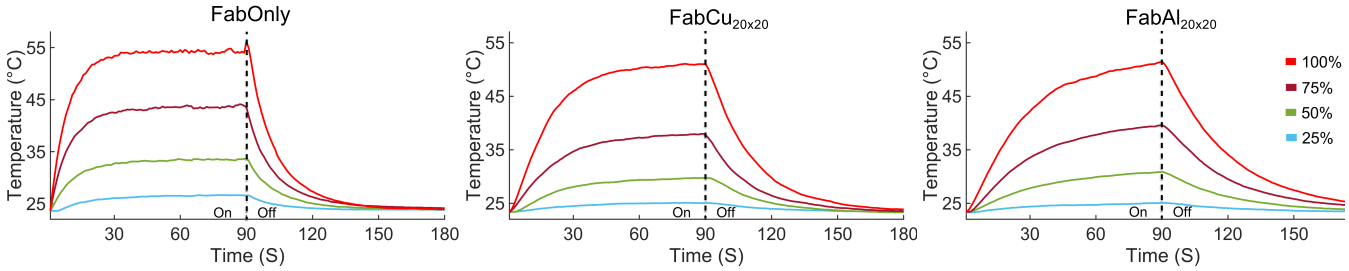

Figure 8: Display temperature change under different amplitude (frequency: 200 Hz)

Disagree, 10: Strongly Agree). The mean scores are shown in Figure 9 (b). A one-way ANOVA with repeated measures was conducted, and significant differences were found between *FabOnly* and $FabCu_{20\times20}$ ($p < 0.001$) as well as *FabOnly* and $FabAl_{20\times20}$ ($p < 0.001$). These results indicate that participants were clearly able to perceive the thermal sensations with $FabCu_{20\times20}$ and $FabAl_{20\times20}$ but not with *FabOnly*.

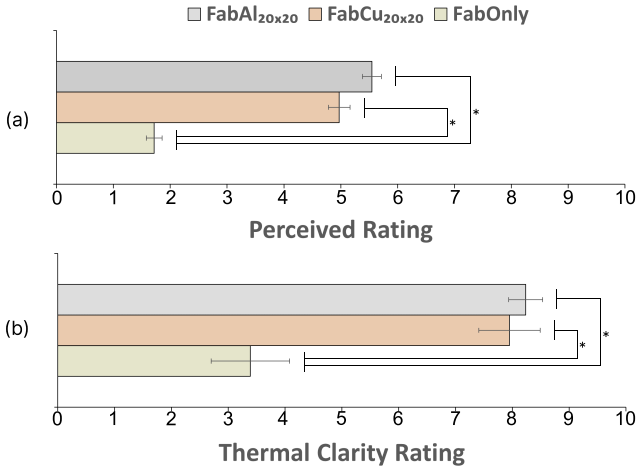

Figure 9: Mean perceived (a) intensity ratings and (b) thermal clarity ratings of thermal stimulus for all three displays.

4.2 User Study 2: Thermal Level Identification

The goal of user study 2 is to evaluate the thermal identification of different temperature levels in each display.

Participants. Twelve participants who did not participate in the previous user study were recruited to participate in this study (5 females; mean age = 25.7 years old; SD = 2.5 years old). All of them were right-handed, and none reported any disorder affecting the sensations of their hands. Each participant was paid a $10 gift card for their participation.

Experimental Conditions. We designed a two-factor experiment: thermal display and temperature levels. For thermal display, we used the same three thermal displays from user study 1: *FabOnly*, $FabCu_{20\times20}$, and $FabAl_{20\times20}$. For temperature levels, we used three levels based on the amplitude of the ultrasonic cues instead of fixed temperature levels because different material has slightly different thermal properties. *Low* (26.6° for *FabOnly*, 25.1°C for $FabCu_{20\times20}$, and 25.0°C for $FabAl_{20\times20}$), *Medium* (43.5°C for *FabOnly*, 37.8°C for $FabCu_{20\times20}$ and 39.6°C for $FabAl_{20\times20}$, and *High* (54.0°C for *FabOnly*, 51.0°C for $FabCu_{20\times20}$, and 51.5°C for $FabAl_{20\times20}$. The temperature levels at each thermal display were determined based on their thermal characteristics with different amplitude of ultrasound cues (see Figure 8). This resulted in a total of $3 \times 3 = 9$ experimental conditions, and each condition was repeated twice, resulting in a total of 18 trials. Similar to the previous experiment, an initial charging time of 60 seconds was required for the display to reach its steady state. The order of the trials was counterbalanced using Latin squares.

Procedure. Participants were briefed about the experimental procedure prior to starting the experiment. Similar to user study 1, their initial skin temperature was measured at the beginning of each trial. The fabric was placed on top of the material holder at a distance of 200 *mm* from the ultrasound display. The ultrasound display was set to a frequency of 200 Hz, and the focal point intensity was set to maximum. A focal point of diameter 10 *mm* was created in the center of the display. For each trial, three thermal stimuli of all three temperature levels (i.e., Low, Medium, and High) were presented in ascending order for the selected display. For each thermal stimulus, the ultrasound display was activated until the temperature of the display was stabilized at its particular temperature level. When the temperature of the display reached a particular temperature level, participants were asked to place an index of their dominant hand inside the white square marked on each display for five seconds. After trying all three thermal stimuli, participants are then asked to try one randomly selected temperature level by placing the index finger for another 5 seconds. Then, they were asked to identify which of the three temperature levels the presented stimulus was by verbally reporting to the experimenter, who then noted the answer on a computer. The order of thermal display was randomized and balanced across participants. The duration of the experiment was about 60 minutes for each participant. The experiment room temperature was maintained at 23.5°C.

Results and Discussion. Figure 10 shows the normalized confusion matrices presenting the mean identification accuracy of temperature levels (Low, Medium, and High) for *FabOnly*, $FabCu_{20\times20}$, and $FabAl_{20\times20}$. The vertical axis denotes the presented condition, and the horizontal axis denotes participant responses. On average, accuracies were 62.50%, 95.83%, and 95.83%, for *FabOnly*, $FabCu_{20\times20}$, and $FabAl_{20\times20}$, respectively. Pairwise Fisher's test showed that this difference in performance was statistically significant between *FabOnly* and $FabCu_{20\times20}$ ($p < 0.001$) as well as *FabOnly* and $FabAl_{20\times20}$ ($p < 0.001$). There was no significance found between $FabCu_{20\times20}$ and $FabAl_{20\times20}$ ($p = 1$). The findings show that when $FabCu_{20\times20}$ and $FabAl_{20\times20}$ were used, the participants were able to identify between temperature levels with clarity, but they were unsure when *FabOnly* was used.

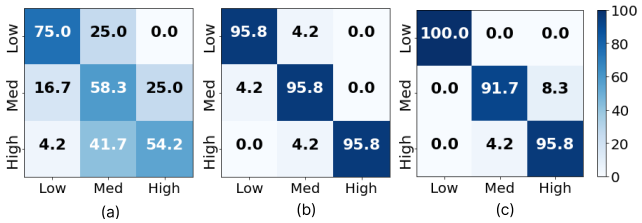

Figure 10: Normalized confusion matrices showing mean identification accuracy for (a) FabOnly, (b) FabCu$_{20\times20}$, and (c) FabAl$_{20\times20}$.

5 Use Cases

We integrated our thermal display employing polyester with aluminum into the central region of an elastic polyester glove to explore use cases and validate our approach (see Figure 12). We chose *FabAl*$_{20\times20}$ thermal display as it performed the best in previous user studies. The fabric side of the thermal display is exposed to the outside environment, while the aluminum is in contact with the skin. Three VR applications were created using a leap motion hand tracking device to precisely target the ultrasound energy towards the interaction area, specifically the palm. At the same time, distinct haptic schemes were generated based on the specific scenario. An initial charging time of 90 seconds to reach the temperature to a steady state is required before interacting with the VR scenes. This initial charging time of 90 seconds is required (instead of 60 seconds for experiments) because the skin has a much higher heat capacity (3390 $J/kg.K$) than the materials (1.1 $J/kg.K$ for polyester and 887 $J/kg.K$ for aluminum). Since the users need to wear a glove and their skin is in contact with the display, overall heat capacity is increased, requiring a longer time to reach a steady state. However, this initial charging time is required only once, and they can interact freely across any VR scenes after the initial charging.

Water Faucet. The first application demonstrated a bathroom scenario with a user interacting with a faucet dispensing hot water (see Figure 11 (a)). During this interaction, a user can move their hands in an upward and downward motion, allowing them to perceive the presence of the water on their palms. For this scene, a circular ultrasound cue with a radius of 10 mm is provided on the user's palm at the location of the collision between the water stream and the hand. The intensity of the haptic scheme was set to 85%, and the frequency was set to 200Hz. The temperature on the surface of the thermal display was estimated to be 48°C based on the haptic intensity and frequency values. We created this use case to demonstrate the practicality and applicability of our approach in situations that necessitate a larger and consistent haptic experience accompanied by apparent thermal sensations.

Hot Coffee. In this scene, a user can interact with some visible fumes rising from the coffee cup (see Figure 11 (b)). The user can place their hands in any manner that intersects with the fumes. To enhance the sensory experience, a discreet and dispersed haptic scheme was generated within the region where the palm intersects with the fumes. The intensity of the haptic scheme was deliberately set at 70% with 200 Hz of frequency to provide a gentle, warm sensation to the user. The temperature on the surface of the thermal display was estimated to be 40°C (based on the haptic intensity and frequency values). A circular sensation, characterized by a variable radius between 10 mm and 20 mm, moves along the interaction area following an unpredictable trajectory. This use case effectively exemplifies the application of the prototype in scenarios where subtle and scattered haptic feedback is synergetically combined with light and subtle thermal cues.

Burning Candle. In this particular use case, a user was engaged in an interaction with a candle flame (see Figure 11 (c)). By placing their hands at various heights, users can perceive temperature changes. For this experience, a dynamic haptic scheme was implemented specifically for the palm area. The intensity of the haptic scheme is set at 100% and 200Hz. The temperature on the surface of the thermal display was estimated to be 53°C based on the haptic intensity and frequency values. The haptic scheme exhibited fluctuations in intensity, reaching the maximum level, while the radius of the haptic cues varied between 10 mm and 15 mm. These fluctuations occur at a rate of 2 times per second, ensuring a rapid and responsive feedback mechanism. The chosen example effectively demonstrates the practicality and functionality of the prototype when presented with the requirement for strong and focused haptic cues.

6 Discussion & Conclusion

This study presented a fabric-based thermal display made of highly absorbent and thermally-conductive materials. It uses an ultrasound haptic display as an external non-contact energy source to generate heat energy and transfer heat to the skin through thermally-conductive materials. We investigated the thermal characteristics of five different fabrics by varying frequencies and amplitudes of the focused ultrasound cues. We found that polyester showed the largest heat absorption and retention. We further investigated the performance of two conductive materials (copper and aluminum) with two sizes (20 mm and 40 mm). Data showed that a size of 20 mm thermally-conductive materials reached higher temperatures. We also compared *FabCu*$_{20\times20}$ and *FabAl*$_{20\times20}$ with *FabOnly* for thermal perception and thermal level identification. We found that the participants perceived the thermal sensations more clearly and with higher intensity with *FabCu*$_{20\times20}$ and *FabAl*$_{20\times20}$. We also showed that our approach is capable of providing distinct temperature levels with a very high identification rate (95.8%) with both *FabCu*$_{20\times20}$ and *FabAl*$_{20\times20}$, as compared to 62.5% of *FabOnly*. Overall, we showed that our thermal display prototype could deliver clear, strong, and distinguishable thermal feedback.

Another strength of our approach is thermal controllability. We showed that temperature levels could be controlled by adjusting the amplitude of the focused ultrasound cues, and we further demonstrated its feasibility to provide clear thermal perception and identification through a set of user studies. All participants reported clear thermal perception on *FabCu*$_{20\times20}$ and *FabAl*$_{20\times20}$, while poor thermal perception on *FabOnly* was observed as they mentioned in the questionnaire: *It mostly gives a neutral feeling.* It clearly shows that our approach of combining thermally-conductive materials can improve thermal transfer efficiency and convey the energy absorbed in fibrous material. With a high identification rate of *FabCu*$_{20\times20}$ and *FabAl*$_{20\times20}$ displays, we proved controllable thermal stimuli through our approach and can be further implemented to achieve enriched thermal sensation.

Our approach has a simple design, making the materials easy to get and modify. The thermal display we propose is flexible and lightweight, and it can provide a seamless experience for the user to grasp and manipulate thermal objects,

Figure 11: Three VR scenes with different rendering schemes: (a) water faucet, (b) hot coffee cup, and (c) burning candle.

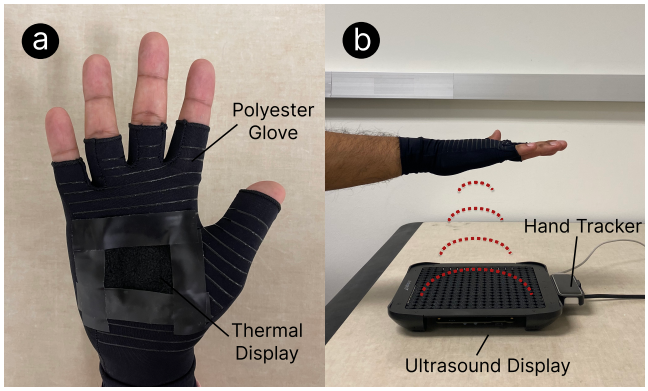

Figure 12: (a) The thermal display embedded on a glove and (b) set up with a Leap Motion hand tracker and ultrasound haptic display.

which can be difficult to achieve with traditional contact-based approaches like Peltiers. The polyester can fit various body parts and is safe for direct skin contact, making it an ideal material for thermal contact display worn on different body parts. Both copper and aluminum displays showed high thermal performance with similar thermal characteristics, and they are flexible and safe for direct skin contact. However, aluminum is considerably less expensive than copper, making it more desirable, especially in large-scale implementation.

We showed the potential application using our approach with proper haptic scheme rendering, which could provide an enriched haptic pattern and thermal level on the palm. We further explored some use cases of our thermal display with a thermal glove and three VR applications to validate our approach. We showcased a moderate thermal sensation with larger and consistent haptic feedback, subtle thermal sensations with weak and scattered haptic feedback, and high temperature with strong and focused haptic feedback on demonstrating the strengths and weaknesses of our approach.

We also identified some limitations. The ultrasound phased array has a limited workspace with an effective range of 200 mm, which would restrict the movement range when wearing the display. Since the range of the ultrasound board is a limiting factor, a better experience can be achieved by making changes to the hardware setup, such as using a more powerful ultrasound haptic display or multiple displays from different angles and directions to widen the interaction space.

Another limitation of this approach is that despite good controllability of temperature levels, it takes a relatively long time to reach a steady state. This initial charging time was approximately 60 seconds to reach the steady state during the experiment and 90 seconds for the use case scenarios. It took more time with the use case scenarios as it requires the thermal display (i.e., aluminum) in the glove to be in contact with the skin at all times, requiring more time to charge the high heat capacity of human skin (3390 $J/kg.K$) and resulting in higher charging time (RC) as shown in Section 2.1. Additionally, there is a thermal perception latency of 0.5 - 2 seconds, which further increases the time to perceive thermal feedback. We believe the heating process can be expedited with more transducers (i.e., increase the capacity of heat generation) and optimized material design (e.g., customized metal shape with lower thermal resistance and adequate metal mass for heat storage). We plan to extend this work to explore thermal display characteristics such as metal size, fibrous material depth, and attachment methods.

Acknowledgements

This work was supported by Electronics and Telecommunications Research Institute (ETRI) grant funded by the Korean government [23ZH1300, Research on Hyper-Realistic Interaction Technology for Five Senses and Emotional Experience] and [23ZS1300, Research on High Performance Computing Technology to Overcome Limitations of AI processing].

References

[1] N. Ranasinghe, P. Jain, N. Thi Ngoc Tram, K. C. R. Koh, D. Tolley, S. Karwita, L. Lien-Ya, Y. Liangkun, K. Shamaiah, C. Eason Wai Tung *et al.*, "Season traveller: Multisensory narration for enhancing the virtual reality experience," in *Proceedings of the 2018 CHI Conference on Human Factors in Computing Systems*, 2018, pp. 1–13.

[2] K. Ragozin, G. Chernyshov, and K. Kunze, "Heatsense – thermal sensory supplementation for superhuman sports," in *2019 IEEE Conference on Virtual Reality and 3D User Interfaces (VR)*, 2019, pp. 1831–1833.

[3] R. L. Peiris, W. Peng, Z. Chen, L. Chan, and K. Minamizawa, "Thermovr: Exploring integrated thermal haptic feedback with head mounted displays," in *Proceedings of the 2017 CHI Conference on Human Factors in Computing Systems*, 2017, pp. 5452–5456.

[4] L. A. Jones and S. J. Lederman, *Human hand function*. Oxford university press, 2006.

[5] S. Gallo, L. Cucu, N. Thevenaz, A. Sengül, and H. Bleuler, "Design and control of a novel thermo-tactile multimodal display," in *2014 IEEE Haptics Symposium (Haptics)*. Ieee, 2014, pp. 75–81.

[6] G.-H. Yang, K.-U. Kyung, M. A. Srinivasan, and D.-S. Kwon, "Quantitative tactile display device with pin-array type tactile feedback and thermal feedback," in *Proceedings 2006 IEEE International Conference on Robotics and Automation, 2006. ICRA 2006.* IEEE, 2006, pp. 3917–3922.

[7] P. Kammermeier, A. Kron, J. Hoogen, and G. Schmidt, "Display of holistic haptic sensations by combined tactile and kinesthetic feedback," *Presence: Teleoperators & Virtual Environments*, vol. 13, no. 1, pp. 1–15, 2004.

[8] P.-H. Han, Y.-S. Chen, K.-C. Lee, H.-C. Wang, C.-E. Hsieh, J.-C. Hsiao, C.-H. Chou, and Y.-P. Hung, "Haptic around: multiple tactile sensations for immersive environment and interaction in virtual reality," in *Proceedings of the 24th ACM symposium on virtual reality software and technology*, 2018, pp. 1–10.

[9] A. Delazio, K. Nakagaki, R. L. Klatzky, S. E. Hudson, J. F. Lehman, and A. P. Sample, *Force Jacket: Pneumatically-Actuated Jacket for Embodied Haptic Experiences*. New York, NY, USA: Association for Computing Machinery, 2018, p. 1–12. [Online]. Available: https://doi.org/10.1145/3173574.3173894

[10] R. L. Peiris, W. Peng, Z. Chen, L. Chan, and K. Minamizawa, "Thermovr: Exploring integrated thermal haptic feedback with head mounted displays," in *Proceedings of the 2017 CHI Conference on Human Factors in Computing Systems*, ser. CHI '17. New York, NY, USA: Association for Computing Machinery, 2017, p. 5452–5456. [Online]. Available: https://doi.org/10.1145/3025453.3025824

[11] A. El Ali, X. Yang, S. Ananthanarayan, T. Röggla, J. Jansen, J. Hartcher-O'Brien, K. Jansen, and P. Cesar, "Thermalwear: Exploring wearable on-chest thermal displays to augment voice messages with affect," in *Proceedings of the 2020 CHI Conference on Human Factors in Computing Systems*, ser. CHI '20. New York, NY, USA: Association for Computing Machinery, 2020, p. 1–14. [Online]. Available: https://doi.org/10.1145/3313831.3376682

[12] H. Son, H. Wang, Y. Singhal, and J. R. Kim, "Upper body thermal referral and tactile masking for localized feedback," *IEEE Transactions on Visualization and Computer Graphics*, vol. 29, no. 5, pp. 2211–2219, 2023.

[13] Z. Dughaish, "Lead telluride as a thermoelectric material for thermoelectric power generation," *Physica B: Condensed Matter*, vol. 322, no. 1-2, pp. 205–223, 2002.

[14] S. Riffat and X. Ma, "Improving the coefficient of performance of thermoelectric cooling systems: a review," *International journal of energy research*, vol. 28, no. 9, pp. 753–768, 2004.

[15] S. Günther, F. Müller, D. Schön, O. Elmoghazy, M. Mühlhäuser, and M. Schmitz, "Therminator: Understanding the interdependency of visual and on-body thermal feedback in virtual reality," in *Proceedings of the 2020 CHI Conference on Human Factors in Computing Systems*, 2020, pp. 1–14.

[16] T. Han, F. Anderson, P. Irani, and T. Grossman, "Hydroring: Supporting mixed reality haptics using liquid flow," in *Proceedings of the 31st Annual ACM Symposium on User Interface Software and Technology*, ser. UIST '18. New York, NY, USA: Association for Computing Machinery, 2018, p. 913–925. [Online]. Available: https://doi.org/10.1145/3242587.3242667

[17] N. Ranasinghe, P. Jain, N. Thi Ngoc Tram, D. Tolley, Y. Liangkun, C. Eason Wai Tung, C. C. Yen, E. Y.-L. Do, K. C. R. Koh, and K. Shamaiah, "A demonstration of season traveller: Multisensory narration for enhancing the virtual reality experience," in *Extended Abstracts of the 2018 CHI Conference on Human Factors in Computing Systems*, ser. CHI EA '18. New York, NY, USA: Association for Computing Machinery, 2018, p. 1–4. [Online]. Available: https://doi.org/10.1145/3170427.3186513

[18] Y. Singhal, H. Wang, H. Gil, and J. R. Kim, "Mid-air thermo-tactile feedback using ultrasound haptic display," in *Proceedings of the 27th ACM Symposium on Virtual Reality Software and Technology*, ser. VRST '21. New York, NY, USA: Association for Computing Machinery, 2021. [Online]. Available: https://doi.org/10.1145/3489849.3489889

[19] D. Iwai, M. Aoki, and K. Sato, "Non-contact thermo-visual augmentation by ir-rgb projection," *IEEE Transactions on Visualization and Computer Graphics*, vol. 25, no. 4, pp. 1707–1716, 2019.

[20] L. Plaghki and A. Mouraux, "How do we selectively activate skin nociceptors with a high power infrared laser? physiology and biophysics of laser stimulation," *Neurophysiologie Clinique/Clinical Neurophysiology*, vol. 33, no. 6, pp. 269–277, 2003. [Online]. Available: https://www.sciencedirect.com/science/article/pii/S0987705303000753

[21] T. Kamigaki, S. Suzuki, and H. Shinoda, "Mid-air thermal display via high-intensity ultrasound," in *SIGGRAPH Asia 2020 Emerging Technologies*, 2020, pp. 1–2.

[22] ——, "Noncontact thermal and vibrotactile display using focused airborne ultrasound," in *International Conference on Human Haptic Sensing and Touch Enabled Computer Applications*. Springer, 2020, pp. 271–278.

[23] Q. ZHU, T. KAMIGAKI, Y. MASUDA, M. FUJIWARA, Y. MAKINO, and H. SHINODA, "Noncontact heat presentation for whole body using high-intensity airborne ultrasound."

[24] T. Iwamoto, M. Tatezono, and H. Shinoda, "Non-contact method for producing tactile sensation using airborne ultrasound," in *International Conference on Human Haptic Sensing and Touch Enabled Computer Applications*. Springer, 2008, pp. 504–513.

[25] T. Carter, S. A. Seah, B. Long, B. Drinkwater, and S. Subramanian, "Ultrahaptics: multi-point mid-air haptic feedback for touch surfaces," in *Proceedings of the 26th annual ACM symposium on User interface software and technology*, 2013, pp. 505–514.

[26] H. Motoyama, M. Fujiwara, T. Morisaki, H. Shinoda, and Y. Makino, "Touchable cooled graphics: Midair 3d image with noncontact cooling feedback using ultrasound-driven mist vaporization," in *SIGGRAPH Asia 2022 Emerging Technologies*, ser. SA '22. New York, NY, USA: Association for Computing Machinery, 2022. [Online]. Available: https://doi.org/10.1145/3550471.3558402

[27] E. M. Samsudin, L. H. Ismail, and A. A. Kadir, "A review on physical factors influencing absorption performance of fibrous sound absorption material from natural fibers," *ARPN Journal of Engineering and Applied Sciences*, vol. 11, no. 6, pp. 3703–11, 2016.

[28] X. Tang and X. Yan, "Acoustic energy absorption properties of fibrous materials: A review," *Composites Part A: Applied Science and Manufacturing*, vol. 101, pp. 360–380, 2017. [Online]. Available: https://www.sciencedirect.com/science/article/pii/S1359835X17302609

[29] U. Berardi and G. Iannace, "Predicting the sound absorption of natural materials: Best-fit inverse laws for the acoustic impedance and the propagation constant," *Applied Acoustics*, vol. 115, pp. 131–138, 2017. [Online]. Available: https://www.sciencedirect.com/science/article/pii/S0003682X16302377

[30] M. Delany and E. Bazley, "Acoustical properties of fibrous absorbent materials," *Applied Acoustics*, vol. 3, no. 2, pp. 105–116, 1970. [Online]. Available: https://www.sciencedirect.com/science/article/pii/0003682X70900319

[31] T. Yang, L. Hu, X. Xiong, M. Petrů, M. T. Noman, R. Mishra, and J. Militký, "Sound absorption properties of natural fibers: A review," *Sustainability*, vol. 12, no. 20, 2020. [Online]. Available: https://www.mdpi.com/2071-1050/12/20/8477

[32] F. Kreith and R. M. Manglik, *Principles of heat transfer*.

Cengage learning, 2016.

[33] P. J. Dyck, I. Zimmerman, D. Gillen, D. Johnson, J. Karnes, and P. O'Brien, "Cool, warm, and heat-pain detection thresholds: testing methods and inferences about anatomic distribution of receptors," *Neurology*, vol. 43, no. 8, pp. 1500–1500, 1993.

[34] K. Ivanov, "Subject of temperature control and the main function of thermoregulation of an organism," *Journal of Thermal Biology*, vol. 24, no. 5, pp. 415–421, 1999. [Online]. Available: https://www.sciencedirect.com/science/article/pii/S0306456599000601

[35] I. Darian-Smith and K. O. Johnson, "Thermal sensibility and thermoreceptors," *Journal of Investigative Dermatology*, vol. 69, no. 1, pp. 146–153, 1977. [Online]. Available: https://www.sciencedirect.com/science/article/pii/S0022202X15450778

[36] F. Bird, J. House, and M. J. Tipton, "The physiological response on immersion in cold water and the cooling rates on swimming in a group of children aged 10–11 years," *International Journal of Aquatic Research and Education*, vol. 9, no. 2, p. 7, 2015.